Journal of Pediatric Surgery 57 (2022) 158–165

Contents lists available at ScienceDirect

Journal of Pediatric Surgery

journal homepage: www.elsevier.com/locate/jpedsurg.org

RNA-sequencing identifies novel transcriptomic signatures in intestinal failure-associated liver disease

Lu Jiang[a,c,d], Nan Wang[a], Siyang Cheng[b,c,d], Yang Liu[b,c,d], Shanshan Chen[a], Ying Wang[a,c,*], Wei Cai[a,b,c,d,**]

[a] Division of Pediatric Gastroenterology and Nutrition, Xinhua Hospital, School of Medicine, Shanghai Jiao Tong University, Shanghai, China
[b] Department of Pediatric Surgery, Xinhua Hospital, School of Medicine, Shanghai Jiao Tong University, Shanghai, China
[c] Shanghai Key Laboratory of Pediatric Gastroenterology and Nutrition, Shanghai, China
[d] Shanghai Institute for Pediatric Research, Shanghai, China

ARTICLE INFO

Article history:
Received 8 July 2021
Revised 6 December 2021
Accepted 6 December 2021

Keywords:
Parenteral nutrition
Transcriptomics
Hes6
Bile acids
Metabolome

ABSTRACT

Background: Total parenteral nutrition (TPN) dependence leads to development of intestinal failure-associated liver disease (IFALD). The spectrum of diseases ranges from cholestasis, steatosis, fibrosis, and cirrhosis that causes significant morbidity. Understanding the disease at molecular level helps us to develop therapeutic targets. We performed transcriptomic analysis on liver from rats with TPN administration, and we assessed the role of selected differentially expressed genes (DEGs), functional pathways, transcriptional factors, and their associations with pathological parameters of IFALD.

Methods: Sprague-Dawley rats were subjected to TPN or standard chow with 0.9% saline for 7 days as controls. RNA-seq analysis was performed on liver samples. Correlations between transcriptional factor hairy and enhancer of split 6 (Hes6) and pathological parameters of IFALD were investigated.

Results: We provided a comprehensive transcriptomic analysis to identify DEGs and functional pathways in liver from TPN-fed rats. We identified solute carrier family 7 member 11 (*Slc7a11*) as the most up-regulated mRNA, and ferroptosis-associated pathways were enriched in TPN group. Transcriptional factor (TF) analysis revealed that Hes6 interacted with Nr1d1, Tfdp2, Zbtb20, and Hmgb2l1. TF target gene prediction analysis suggested that Hes6 may regulate genes associated with bile acid secretion and fatty acid metabolism. Last, hepatic *Hes6* expression was significantly decreased in TPN-fed rats, and was positively correlated with several taurine-conjugated bile acids and negatively correlated with hepatic triglyceride level.

Conclusions: RNA-seq analysis revealed unique transcriptomic signatures in the liver following TPN administration. Hes6 may be a critical regulator for IFALD pathogenesis.

What is known:

• Total parenteral nutrition (TPN) is associated with development of hepatic steatosis and cholestasis. Transcriptional factor Hes6 prevents hepatic lipid accumulation in a mouse model of NAFLD.

• RNA-seq reveals alteration of ferroptosis-associated genes and pathways in response to TPN. Reduced expression of *Hes6* was associated with dysregulation of bile acid and lipid metabolism in a rat model of IFALD.

1. Introduction

Intestinal failure-associated liver disease (IFALD) refers to liver dysfunction caused by long-term dependence of parenteral nutrition (PN) in patients with intestinal failure [1]. The clinical spectrum of IFALD mainly include steatosis, cholestasis, and gallbladder sludge/stones [2]. To date, the mechanisms underlying IFALD development are poorly understood, and there is no effective therapy other than discontinuing PN. In pediatric patients with short

Abbreviations: COG, clusters of orthologous groups of proteins; DEG, differentially expressed gene; FDR, false discovery rate; GO, gene ontology; Hes6, hairy and enhancer of split 6; IFALD, intestinal failure-associated liver disease; SBS, short bowel syndrome; TF, transcriptional factor; TPN, total parenteral nutrition.

* Corresponding author at: Division of Pediatric Gastroenterology and Nutrition, Xinhua Hospital, School of Medicine, Shanghai Jiao Tong University, 1665 Kong Jiang Road, 200092, Shanghai, China.

** Corresponding author at: Department of Pediatric Surgery, Xinhua Hospital, School of Medicine, Shanghai Jiao Tong University; Shanghai Institute for Pediatric Research, 1665 Kong Jiang Road, 200092, Shanghai, China.

E-mail addresses: wangying02@xinhuamed.com.cn (Y. Wang), caiw1978@163.com (W. Cai).

https://doi.org/10.1016/j.jpedsurg.2021.12.015
0022-3468/

bowel syndrome (SBS) and intractable diarrhea, Ohkohchi et al. observed a significant increase in fecal bile acid excretion and altered bile acid composition [3]. Further, altered bile acid metabolism and FXR signaling are demonstrated in animal models of IFALD, targeting which could be therapeutically beneficial [4,5]. To better understand the disease at transcriptional level, we performed RNA-seq analysis using liver samples from control and rats that received total parenteral nutrition (TPN). By combining the transcriptomic analysis with metabolomics on serum bile acids, we identified a critical transcriptional factor hairy and enhancer of split 6 (Hes6) in IFALD. Further, we showed that hepatic *Hes6* expression was decreased in rats with IFALD, and it was predicted to regulate bile acid- and lipid metabolism-associated genes. Last, hepatic *Hes6* expression was positively correlated with several taurine-conjugated bile acids, suggesting that Hes6 could be an important regulator for IFALD pathogenesis by regulating bile acid profile and lipid metabolism. Taken together, we provided a detailed hepatic transcriptomic analysis in a rat model of IFALD, in which we identified Hes6 as a potential central regulator of bile acid homeostasis and lipid metabolism.

2. Methods

2.1. Animals

Male Sprague-Dawley rats purchased from Shanghai Laboratory Animal Center (Shanghai, China) at the age of 4 weeks were subjected to 0.9% saline with standard chow (control group, n=12), TPN for 7 days (n=16), or TPN for 14 days (n=4) as previously described [6]. Briefly, a central venous catheter (CVC) was inserted into superior vena cava through the right jugular vein. The TPN solution was sterilized and replaced daily as an all-in-one balanced mixture of 8.5% amino acids, lipids (20% medium-chain triglyceride/long-chain triglyceride, Lipofundin), 50% dextrose, electrolytes, trace elements, and vitamins with a nonprotein calorie to nitrogen ratio of 295:1 as previously summarized [6]. All animal studies were approved by the Experimental Animal Care and Use Committee of Shanghai Jiao Tong University.

2.2. RNA isolation and RNA sequencing

Total RNA from liver was extracted using TRIzol reagent according to the manufacturer's instruction. Ribosomal RNA was depleted before library preparation. Libraries were constructed and sequenced on Illumina HiSeq 4000 platform (Biomarker Technologies, China). Sequence reads were trimmed and aligned to rat genome (Rnor 6.0) using Tophat2 software [7]. Gene expression levels were estimated using Cufflinks software [8]. Differentially expressed genes (DEGs) were identified using DESeq2 package [9]. Gene expression fold change $\geq$ 1.5 and false discovery rate (FDR) $<$ 0.05 were set as the threshold values for subsequent analysis. Gene ontology (GO) annotations for the genes were obtained by Blast2GO [10]. Gene sequences were also aligned to the Clusters of Orthologous Groups of proteins (COG) database to predict and classify functions [11]. KEGG pathways were assigned to the assembled sequences by perl script. Gene set enrichment analysis (GSEA) was performed with R package clusterProfiler [12]. To identify the active transcriptional factors network, a Bioconductor package CoRegNet was used [13]. Sequence data were registered at NCBI under BioProject PRJNA718087. The accession number for the RNA-seq data reported in this study was GEO: GSE171007.

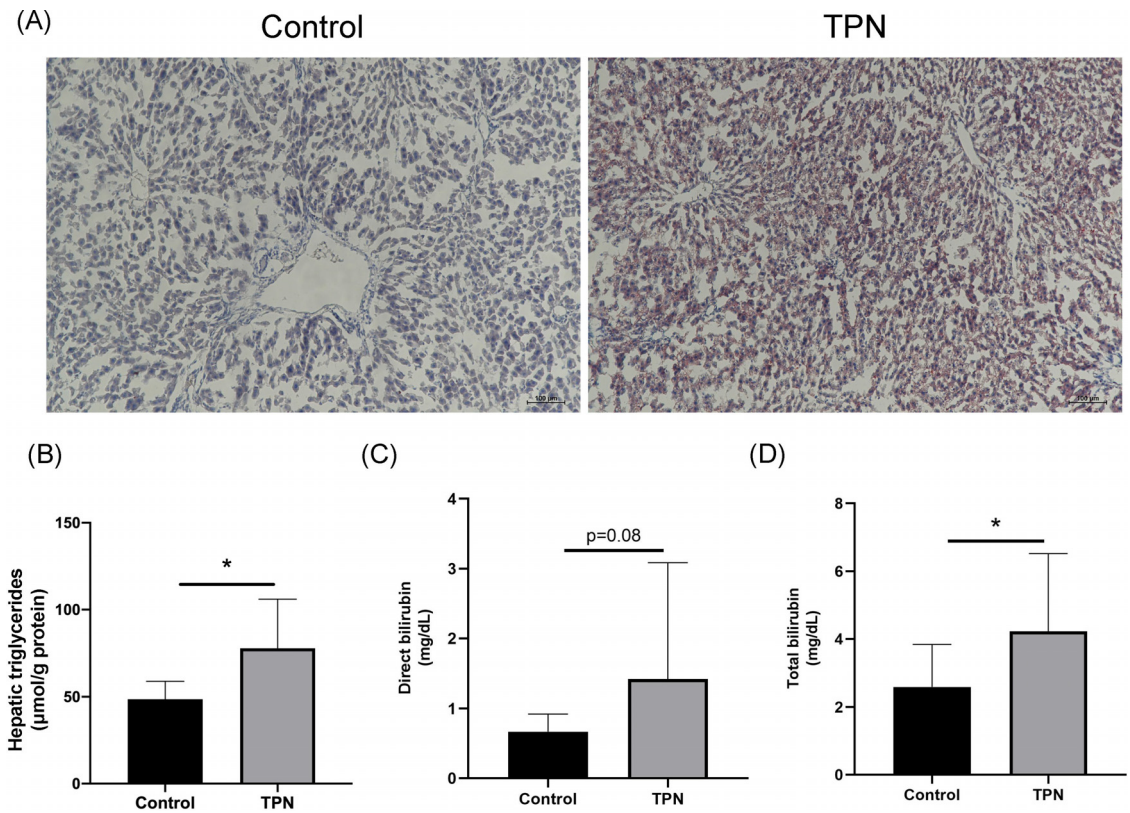

Fig. 1. Characterization of hepatic steatosis and cholestasis in a rat model of IFALD. (A) Oil red O staining on liver sections from the controls and TPN rats. (B-D) Hepatic triglyceride (B), serum direct bilirubin (C), and serum total bilirubin (D) levels in controls and TPN rats. Control group: n=11-16, TPN group: n=11-14. TPN, total parenteral nutrition, $^{*}P<0.05$.

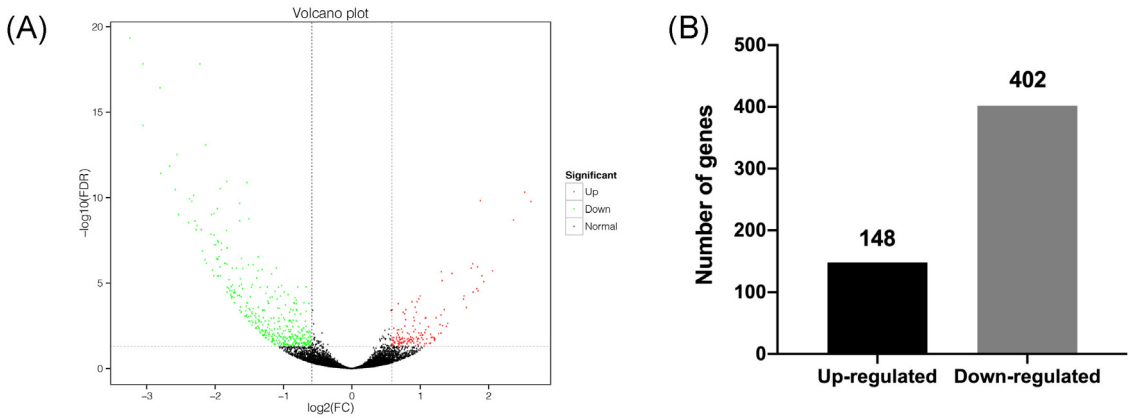

(C)

Gene symbol	FC	FDR	Up/Down
Slc7a11	6.1566525	1.70E-10	up
Mthfd2	5.78106949	4.88E-11	up
Ptprz1	5.1534948	2.02E-09	up
Adm2	4.17481278	1.95E-06	up
Asns	3.82266517	8.15E-06	up
Fut1	3.74205388	3.73E-06	up
Psat1	3.58768226	1.12E-06	up
Slc29a4	3.56070648	2.13E-05	up
Phgdh	3.4289053	3.41E-05	up
Cpt1b	3.41525905	7.40E-07	up
Rrm2	-9.4662359	4.55E-20	down
RGD1564865	-8.2821922	1.54E-18	down
Ect2	-6.9659571	3.76E-17	down
Ccna2	-6.3190658	1.44E-12	down
Tm7sf2	-5.8659495	3.02E-13	down
Cdkn3	-5.7719929	9.58E-10	down
Cenpf	-5.2208948	2.83E-09	down
Hmmr	-5.1770965	1.18E-10	down
Nusap1	-5.0453006	1.65E-10	down
Mki67	-4.9583438	7.54E-11	down

Fig. 2. Differentially expressed genes (DEGs) from RNA-seq analysis in liver in response to total parenteral nutrition (TPN). (A) Volcano plot illustrating DEGs in liver between the controls and TPN rats. (B) Number of up- and down-regulated genes in liver in response of TPN compared with the controls. (C) Top 10 up- and down-regulated genes in TPN rats compared with controls. Cutoff for DEGs is absolute fol change $\geq$ 1.5, false discovery rate (FDR) $<$ 0.05. Control group: n=3, TPN group: n=3.

2.3. Real-Time qPCR

cDNA was generated from total liver RNA, and real-time qPCR was performed as previously described [14]. Primer sequences for *Hes6* were forward 5'-GCTTCGCTGCTGGCTACATCC-3' and reverse 5'- ATGGACTCTAGCAGGTGGTTCAGG-3'. Real-time qPCR was performed using SYBR Premix (Applied Biosystems) on QuantStudio Dx Real-Time instrument (Thermo Fisher).

2.4. Serum bile acid measurement

Serum bile acids from control and TPN-administered rats were analyzed by Waters ACQUITY ultra performance liquid chromatograph (BEH C18l 1.7 μm, 2.1 mm $\times$ 100 mm column) coupled to a Waters Xevo TQ-S triple quadrupole mass spectrometer as previously described [6].

2.5. Lipid content measurement

To determine lipid accumulation, liver sections were embedded into OCT compound, cut at the thickness of 8μm, and stained with Oil red O (Sigma-Aldrich) as previously described [14]. Hepatic triglycerides were measured using a triglyceride assay kit (GPO-POD; Applygen Technologies Inc.).

2.6. Statistical analysis

All data are expressed as mean $\pm$ s.e.m. except stated otherwise. Comparisons between two groups were performed by Student's t test. Spearman's correlation was performed for correlation analysis. Statistical analysis was performed using R statistical software, R version V.3.6.2, 2019 (R Foundation for Statistical Computing) and GraphPad Prism (V.8.4.2). A P value $<$ 0.05 was considered statistically significant.

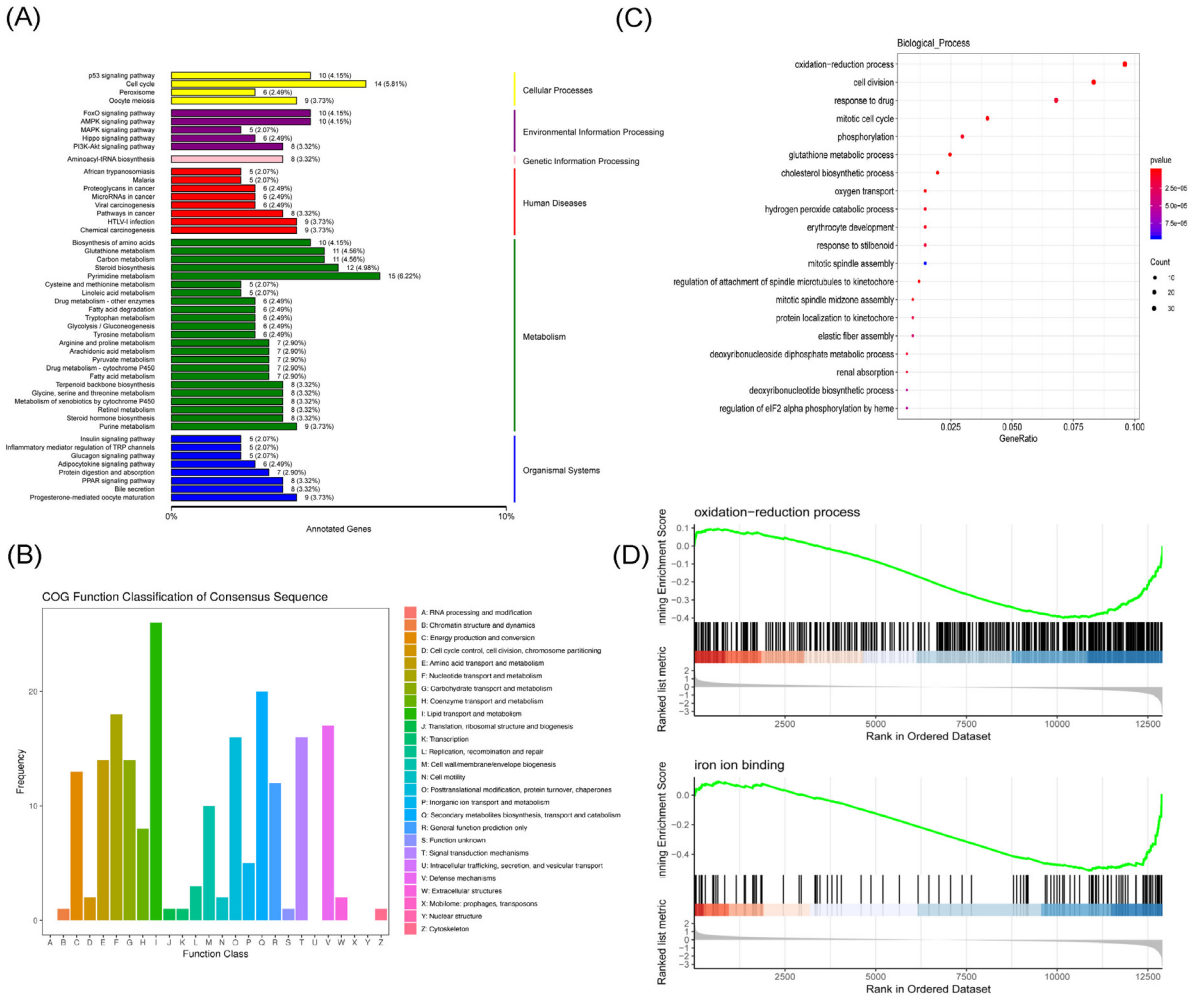

Fig. 3. Functional analysis in liver in response to total parenteral nutrition (TPN). (A) Bar chart of significantly enriched KEGG pathways of differentially expressed genes (DEGs) following TPN treatment. (B) Clusters of Orthologous Groups of proteins (COG) functional classification of DEGs following TPN treatment. (C) Dotplot of top 20 significant gene ontology (GO) biological processes terms of DEGs in response to TPN. (D) GSEA plots of ferroptosis-associated pathways. Control group: n=3, TPN group: n=3.

3. Results

3.1. Characterization of IFALD rat model

After 7 days of total parenteral nutrition (TPN) infusion, we have characterized the development of hepatic steatosis by measuring hepatic triglycerides (TG) and oil red O staining (Fig. 1a-b). Overall, an increased level of lipid accumulation indicating development of hepatic steatosis was observed in TPN group compared with controls. Serum levels of ALT and AST did not differ between TPN and control rats as previously described [6], while direct bilirubin level was trended to increase (Fig. 1c). Last, total bilirubin was significantly increased in rats following TPN treatment (Fig. 1d). These findings suggest that TPN induced hepatic steatosis and moderate cholestasis in rats.

3.2. Liver transcriptomic profile changes in response to TPN in rats

To visualize differentially expressed genes (DEGs) in liver after TPN treatment, we plotted significantly altered genes in a volcano plot (Fig. 2a). In total, we identified 148 up-regulated genes and 402 down-regulated genes when comparing with controls (Fig. 2b). Top ten up- and down-regulated genes are listed in Fig. 2c. Interestingly, *Slc7a11* was the mostly up-regulated gene, suggesting a possible alteration of ferroptosis pathway in TPN-fed rats (Fig. 2c). We further performed functional analysis of DEGs using KEGG (Fig. 3a), COG (Fig. 3b), and GO biological process (Fig. 3c) databases. The subclassification of KEGG pathways include cellular processes, environmental information processing, genetic information processing, human diseases, metabolism, and organismal systems (Fig. 3a). KEGG analysis revealed potentially important roles of cell cycle, AMPK signaling pathway, fatty acid degradation and metabolism, PPAR signaling pathway, and bile secretion pathway in response to TPN (Fig. 3a). Top COG terms of DEGs indicated altered functions of cell cycle and lipid transport and metabolism (Fig. 3b). Top GO terms of DEGs indicated altered functions of oxidation-reduction process, cell cycle, glutathione metabolic process, mitotic cell cycle, and cholesterol biosynthetic process (Fig. 3c). Last, we performed gene set enrichment analysis (GSEA) of to ascertain the function changes in response to TPN. Consistently, ferroptosis-associated pathways such as oxidation-reduction process (GO biological process) and iron ion binding (GO molecular function) were significantly enriched in TPN group (Fig. 3d).

3.3. Transcriptional factor analysis in response to TPN in rats

We further analyzed transcriptional factor (TF) activities based on DEGs in TPN rats in comparison with controls. We per-

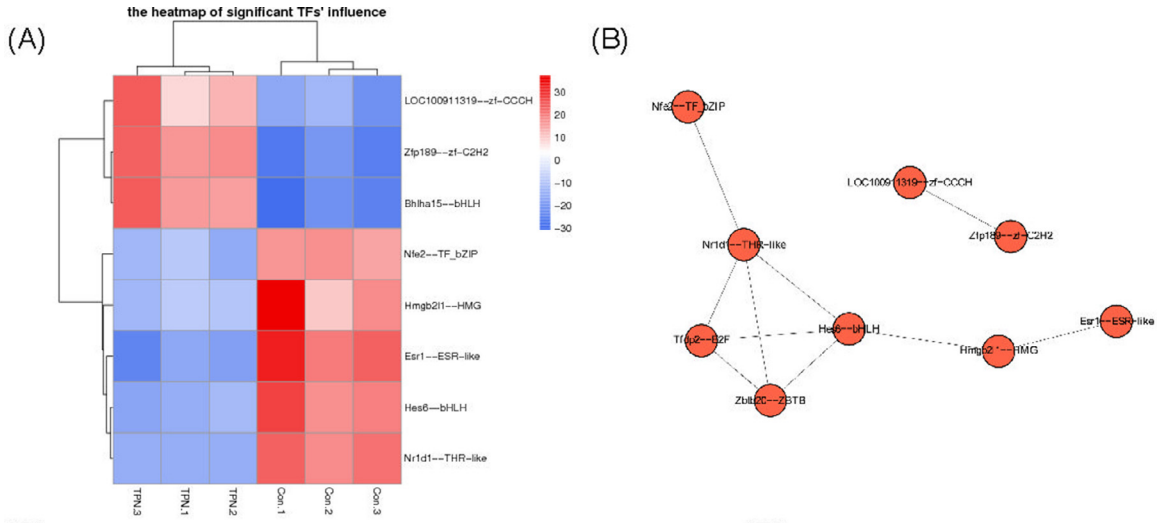

(C)

Reg1	Reg2	Support	Fisher Test	Adjusted *P* value
Hes6--bHLH	Nr1d1–THR-like	0.064045	5.72E-16	2.86E-15
Esr1–ESR-like	Hmgb2l1–HMG	0.035474	4.05E-14	1.52E-13
Hes6--bHLH	Hmgb2l1–HMG	0.035474	5.37E-17	4.02E-16
LOC100911319--zf-CCCH	Zfp189--zf-C2H2	0.023355	1.01E-11	3.02E-11
Tfdp2--E2F	Zbtb20–ZBTB	0.016051	8.65E-60	1.30E-58
Nr1d1–THR-like	Tfdp2--E2F	0.016051	4.88E-09	1.05E-08
Hes6--bHLH	Tfdp2--E2F	0.016051	1.03E-05	1.71E-05
Nr1d1–THR-like	Zbtb20–ZBTB	0.016051	4.88E-09	1.05E-08
Hes6--bHLH	Zbtb20–ZBTB	0.016051	1.03E-05	1.71E-05
Nfe2--TF_bZIP	Nr1d1–THR-like	0.014366	0.001056	0.001584

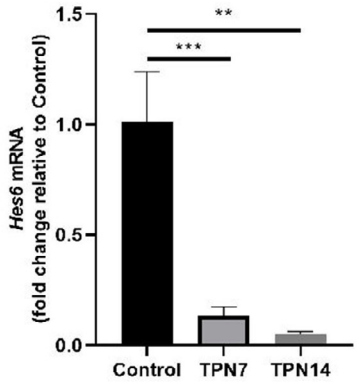

Fig. 4. Transcriptional factor (TF) analysis in liver in response to total parenteral nutrition (TPN). (A) Heatmap showing the clustering profile of TFs in the controls and TPN rats. (B) Networks showing TF-TF interactions. (C) Statistics of TF-TF interaction analysis. (D) Hepatic mRNA level of *Hes6* in controls and TPN rats assessed by real-time qPCR. For A-C, Control group: n=3, TPN group: n=3; For D, Control group: n=12, TPN7 group: n=16, TPN14 group: n=4. Hes6, hairy and enhancer of split 6. $^{*}P < 0.0001$.

formed hierarchical cluster analysis with differentially expressed TFs, in which controls and TPN rats showed similarities respectively within each group (Fig. 4a). Using the R/Bioconductor package CoRegNet [13], we explored the TF-TF co-regulatory network composed of 9 significantly altered TFs linked by co-regulatory interactions, in which Hes6 was shown to interact with Nr1d1, Tfdp2, Zbtb20, and Hmgb2l1 (Fig. 4b-c). To validate the expression level of *Hes6* in liver, we performed real-time qPCR on livers from control and rats administered with TPN for 7 and 14 days. Consistently, *Hes6* expression was significantly decreased after 7 days of TPN infusion compared with the control group, and the expression tended to reduce further at day 14 (Fig. 4d).

3.4. Correlation between hepatic Hes6 *expression and pathological parameters in TPN-fed rats*

Serum bile acids were measured and described previously [6]. Overall, TPN rats were presented as a decreased percentage of primary bile acids and an increased ratio of secondary to primary bile acids. To investigate the role of Hes6 in regulating bile acid profile during IFALD development, we first explored genes associated with bile secretion pathway. Interestingly, all gene expression in the pathway (*Abcc2, Hmgcr, Abcg8, Abcc3, Slco1b2, Sult2a2, Ldlr, and Car2*) was down-regulated in TPN group compared with controls (Fig. 5a). We further cross-examined the genes in bile secretion pathway with predicted Hes6 target genes. The overlapped genes are listed in Fig. 5b. To explore the relationship between Hes6 and serum bile acid signature, we correlated hepatic *Hes6* expression with serum bile acid levels. Interestingly, several taurine-conjugated bile acids, such as TCDCA (R=0.84), TCA (R=0.71), TαMCA (R=0.76), and TUDCA (R=0.68) were positively correlated with *Hes6* expression. Bile acids associated with secondary bile acid synthesis (GLCA/CDCA (R=-0.81), GDCA/CA (R=-0.77), DCA/CA (R=-0.54), TLCA/CDCA (R=-0.51)) were negatively associated with *Hes6* expression (Fig. 5c).

Last, we analyzed significantly enriched KEGG pathways associated with lipid metabolism in TPN rats. Overall, we showed that fatty acid metabolism, fatty acid degradation, and PPAR signaling pathways were enriched in TPN rats by the gene-concept networks (Fig. 6a). Among all genes in these pathways, we noticed that *Cyp4a2, Pck2, Fads2, Fads1, Elovl5, and Acsl1* were predicted as Hes6 targets (Fig. 6b), which is consistent with previous findings that Hes6 prevents hepatic lipid accumulation in mice fed with western diet [15]. Spearman's correlation demonstrated a signifi-

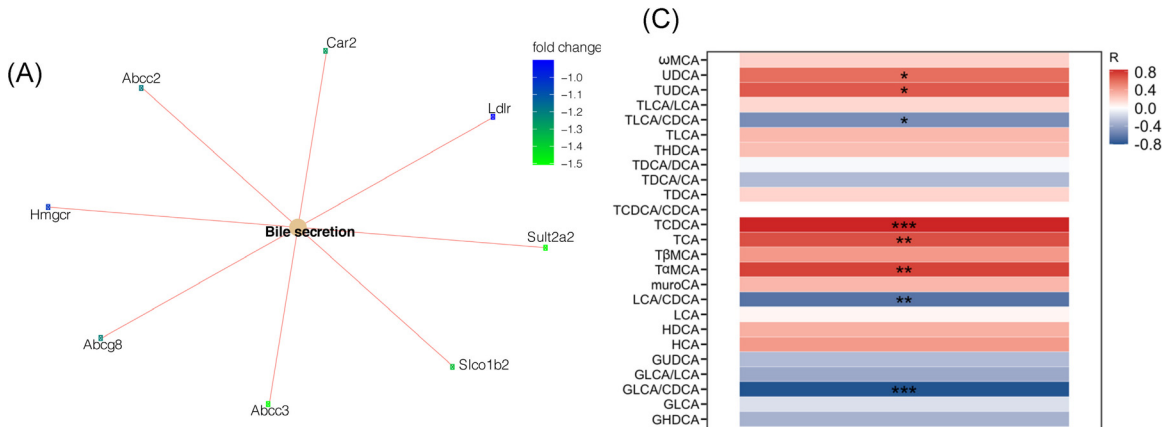

(B)

Gene symbol	FC	FDR	Up/Down
Abcc3	-2.8422884	8.58E-07	down
Abcg8	-2.3205405	0.02066747	down
Car2	-2.4202093	0.00038041	down
Hmgcr	-2.0534312	0.01379349	down
Ldlr	-1.8663116	0.01305772	down

Fig. 5. Correlation between hepatic *Hes6* expression and serum bile acid profiling in IFALD rats. (A) Gene-concept networks of bile secretion pathway. (B) Genes in bile secretion pathways that were predicted as Hes6 targets. (C) Heatmap of Spearman's correlation between hepatic *Hes6* mRNA and serum bile acids. Red color indicates positive correlation, blue color indicates negative correlation. For A-B, Control group: n=3, TPN group: n=3; For C, Control group: n=7, TPN group: n=12. apoCA, apocholic acid; CA, cholic acid; CDCA, chenodeoxycholic acid; DCA, deoxycholic acid; DHCA, dehydrocholic acid; GCA, glycocholic acid; GCDCA, glycochenodexycholic acid; GDCA, glycodeoxycholic acid; GHCA, glycohyocholic acid; GHDCA, glycodehydrocholic acid; GLCA, glycolithocholic acid; GUDCA, glycoursodeoxycholic acid; HCA, hyocholic acid; HDCA, dehydrocholic acid; ketoLCA, keto-lithocholic acid; LCA, lithocholic acid; MCA, muricholic acid; TCA, taurocholic acid; TCDCA, taurochenodeoxycholic acid; TDCA, taurodeoxycholic acid; THDCA, taurodehydrocholic acid; TLCA, taurolithocholic acid; TUDCA, tauroursodeoxycholic acid; UDCA, ursodeoxycholic acid. $^{*}P < 0.05$ $P > 0.01$, $^{**}P < 0.01$ $P > 0.001$, $^{***}P < 0.001$.

cant correlation between *Hes6* expression and hepatic triglyceride level (R=-0.68, Fig. 6c), suggesting a possible association between reduced Hes6 and increased lipid accumulation in IFALD.

4. Discussion

To comprehensively understand the liver transcriptomic profile in IFALD, we performed RNA-seq analysis in TPN rats in comparison with controls. We analyzed DEGs, functional pathways, and transcriptional factor (TF) activities that might contribute to IFALD pathogenesis. By investigating the relationship between transcriptomic profile and IFALD-associated parameters, we identified Hes6 as a potential regulator for bile acid signaling and lipid metabolism.

TPN is associated with hepatic steatosis and dysregulation of bile acid metabolism that may lead to steatosis and cholestasis [6]. In our study, we first characterized the rat model of IFALD after receiving TPN for 7 days, and we confirmed hepatic steatosis and cholestasis as the main pathophysiology. Previous study has investigated the role of TPN in rats for up to 14 days, while no inflammation and fibrosis was detected in addition to steatosis and cholestasis [16]. A variety of studies suggest that high content of phytosterols in soybean oil-based lipid emulsions exhibited toxic effects in both patients and animal models of IFALD, while the addition of alpha-tocopherol may reverse the disease by exhibiting anti-inflammatory effects [17]. At molecular level, the liver transcriptome and associated functional annotations in animal models of IFALD have not been reported yet. In our study, we observed a strong upregulation of cystine/glutamate antiporter xCT (*Slc7a11*) in TPN-fed rats and significant enrichment of ferroptosis-associated pathways, suggesting a possible dysregulation of ferroptosis pathway in response to TPN [18]. Ferroptosis is a form of regulated cell death characterized by iron-dependent accumulation of lipid hydroperoxides up to lethal levels [18]. Dysregulation of ferroptosis has been linked to various liver diseases, such as nonalcoholic steatohepatitis (NASH) [19], ethanol-induced liver injury [20], and liver fibrosis [21]. Therefore, Slc7a11 and ferroptosis could provide attractive therapeutic targets for IFALD. TF activity analysis revealed that Hes6 interacts with multiple significantly activated TFs in IFALD, among which Hes6-Nr1d1 had the highest interaction score. Importantly, previous study demonstrated a critical role of nuclear receptor subfamily 1, group D, member 1 (Nr1d1) in mediating hepatic steatosis, and loss of DNA binding of Nr1d1 in mice was associated with a deterioration in hepatic steatosis [22]. Zinc finger and BTB-domain containing 20 (Zbtb20), another TF that interacts with Hes6, is an important regulator of epidermal growth factor receptor (EGFR) and hepatocyte proliferation. Mice lacking Zbtb20 in hepatocytes exhibited a remarkable defect in liver re-

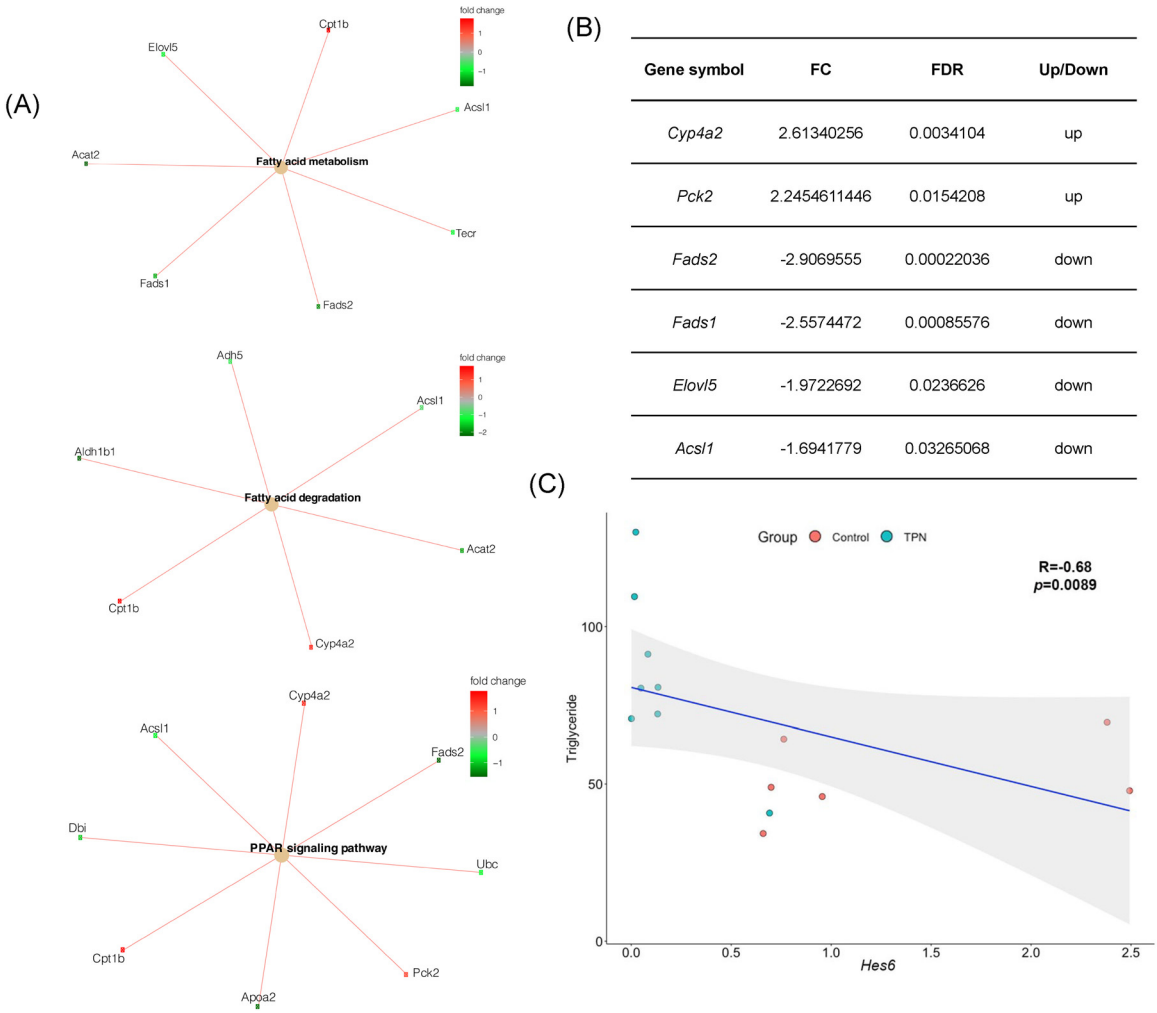

Gene symbol	FC	FDR	Up/Down
Cyp4a2	2.61340256	0.0034104	up
Pck2	2.2454611446	0.0154208	up
Fads2	-2.9069555	0.00022036	down
Fads1	-2.5574472	0.00085576	down
Elovl5	-1.9722692	0.0236626	down
Acsl1	-1.6941779	0.03265068	down

Fig. 6. Correlation between hepatic *Hes6* expression and lipid metabolism in IFALD. (A) Gene-concept networks of lipid metabolism-associated pathways. (B) Genes in lipid metabolism-associated pathways that were predicted as Hes6 targets. (C) Spearman's correlation between *Hes6* expression and hepatic triglycerides level. For A-B, Control group: n=3, TPN group: n=3; For C, Control group: n=6, TPN group: n=8. TPN, total parenteral nutrition; Hes6, hairy and enhancer of split 6.

generation after partial hepatectomy [23]. Whether Hes6 interacts with TFs to co-regulate IFALD requires further investigation. RNA-seq analysis and further validation showed a decreased expression of hepatic *Hes6* in TPN-fed rats. Hes6 was previously studied in a mouse model of nonalcoholic fatty liver disease (NAFLD), in which they showed Hes6 represses peroxisome proliferator-activated receptor gamma 2 (*Pparg2)* gene expression and protects mice from hepatic lipid accumulation induced by western diet [15]. To investigate the role of Hes6 in the pathogenesis of IFALD, we performed Spearman's correlation between hepatic *Hes6* expression and serum bile acid profile. To our surprise, *Hes6* is positively correlated with multiple taurine-conjugated bile acids. We have examined the expression of two key enzymes for bile acid conjugation, bile acid CoA synthase and bile acid CoA-amino acid *N*-acetyltransferase (BAAT) [24], and their expression was not affected in response to TPN (data not shown). As Hes6 was predicted to regulate genes in bile secretion pathway, we speculate that taurine-conjugated bile acid transport could be defected due to a decreased *Hes6* level. Further studies are needed to explore the target genes of Hes6 responsible for taurine-conjugated bile acid synthesis or transportation. Last, we analyzed functions associated with fatty acid homeostasis. Consistent with a known lipid accumulation phenotype in IFALD rat liver [6], fatty acid degradation and metabolism and PPAR signaling pathway were activated in TPN group. As we expected, an inverse correlation between *Hes6* expression and hepatic triglyceride level indicated a possible role of Hes6 in regulating lipid metabolism. Although we did not detect changes in *Pparg* expression, Hes6 could still regulate hepatic steatosis by other unknown mechanisms. Previous studies suggest that lack of enteral feeding results in increased intestinal permeability that facilitates translocation of lipopolysaccharide into liver via portal vein, resulting in liver injury [25]. The impact of absence of enteral feeding on liver transcriptomic profile, especially Hes6 expression, in the settings of IFALD should be evaluated further.

To our knowledge, we present the first comprehensive analysis by integrating liver transcriptomic analysis with metabolomic analysis in a rat model of IFALD. By identifying a critical TF gene Hes6, we proposed that it could be a master regulator for the pathogenesis of IFALD by regulating bile acid homeostasis and lipid metabolism. The limitation of our study was the lack of longer timepoints following TPN administration, so we were not able to investigate the liver transcriptomic profile change over time. In addition, if different lipid emulsions have different effects on Hes6 expression was not explored in our study, or if pig/piglet models of IFALD that resembles patients exhibit different transcriptomic profile remain unknown. Last, as gut microbiome plays an important role in IFALD pathogenesis, how it affects Hes6 expression should be investigated. Future studies should be performed to validate the role of Hes6 in patients and animal models of IFALD. A broader understanding Hes6 may lead to development of therapeutic options.

Funding

This work was supported by National Natural Science Foundation of China (81974066, 81630039), Foundation of Shanghai Municipal Health Commission (Key weak discipline construction project), Foundation of Shanghai Municipal Health Commission (shslczdzk05702), and Foundation of Science and Technology Commission of Shanghai Municipality (19495810500).

Conflict of interest

The authors declare no conflict of interest.

References

[1] Cederholm T, Barazzoni R, Austin P, Ballmer P, Biolo G, Bischoff SC, et al. ESPEN guidelines on definitions and terminology of clinical nutrition. Clin Nutr 2017;36(1):49–64.
[2] Nowak K. Parenteral Nutrition–Associated Liver Disease. Clinical Liver Disease 2020;15(2):59–62.
[3] Ohkohchi N, Andoh T, Izumi U, Igarashi Y, Ohi R. Disorder of bile acid metabolism in children with short bowel syndrome. J Gastroenterol 1997;32(4):472–9.
[4] Lapthorne S, Pereira-Fantini PM, Fouhy F, Wilson G, Thomas SL, Dellios NL, et al. Gut microbial diversity is reduced and is associated with colonic inflammation in a piglet model of short bowel syndrome. Gut Microbes 2013;4(3):212–21.
[5] Jain AK, Stoll B, Burrin DG, Holst JJ, Moore DD. Enteral bile acid treatment improves parenteral nutrition-related liver disease and intestinal mucosal atrophy in neonatal pigs. Am J Physiol Gastrointest Liver Physiol 2012;302(2):G218–24.
[6] Wang N, Wang J, Zhang T, Huang L, Yan W, Lu L, et al. Alterations of gut microbiota and serum bile acids are associated with parenteral nutrition-associated liver disease. J Pediatr Surg 2020.
[7] Kim D, Pertea G, Trapnell C, Pimentel H, Kelley R, Salzberg SL. TopHat2: accurate alignment of transcriptomes in the presence of insertions, deletions and gene fusions. Genome Biol 2013;14(4):R36.
[8] Trapnell C, Williams BA, Pertea G, Mortazavi A, Kwan G, van Baren MJ, et al. Transcript assembly and quantification by RNA-Seq reveals unannotated transcripts and isoform switching during cell differentiation. Nat Biotechnol 2010;28(5):511–15.
[9] Love MI, Huber W, Anders S. Moderated estimation of fold change and dispersion for RNA-seq data with DESeq2. Genome Biol 2014;15(12):550.
[10] Conesa A, Götz S, García-Gómez JM, Terol J, Talón M, Robles M. Blast2GO: a universal tool for annotation, visualization and analysis in functional genomics research. Bioinformatics 2005;21(18):3674–6.
[11] Tatusov RL, Galperin MY, Natale DA, Koonin EV. The COG database: a tool for genome-scale analysis of protein functions and evolution. Nucleic Acids Res 2000;28(1):33–6.
[12] Yu G, Wang LG, Han Y, He QY. clusterProfiler: an R package for comparing biological themes among gene clusters. OMICS 2012;16(5):284–7.
[13] Nicolle R, Radvanyi F, Elati M. CoRegNet: reconstruction and integrated analysis of co-regulatory networks. Bioinformatics 2015;31(18):3066–8.
[14] Duan Y, Llorente C, Lang S, Brandl K, Chu H, Jiang L, et al. Bacteriophage targeting of gut bacterium attenuates alcoholic liver disease. Nature 2019;575(7783):505–11.
[15] Park JE, Lee M, Kim SC, Zhang Y, Hardwick JP, Lee YK. Hairy and enhancer of split 6 prevents hepatic lipid accumulation through inhibition of Pparg2 expression. Hepatol Commun 2017;1(10):1085–98.
[16] Cao X, Feng F, Liu X, Sun C, Yang X, Fang Y, et al. Exogenous Secretin Improves Parenteral Nutrition-associated Liver Disease in Rats. J Pediatr Gastroenterol Nutr 2020;70(4):430–5.
[17] Khalaf RT, Sokol RJ. New Insights Into Intestinal Failure-Associated Liver Disease in Children. Hepatology (Baltimore, Md) 2020;71(4):1486–98.
[18] Stockwell BR, Friedmann Angeli JP, Bayir H, Bush AI, Conrad M, Dixon SJ, et al. Ferroptosis: A Regulated Cell Death Nexus Linking Metabolism, Redox Biology, and Disease. Cell 2017;171(2):273–85.
[19] Qi J, Kim JW, Zhou Z, Lim CW, Kim B. Ferroptosis Affects the Progression of Nonalcoholic Steatohepatitis via the Modulation of Lipid Peroxidation-Mediated Cell Death in Mice. Am J Pathol 2020;190(1):68–81.
[20] Zhou Z, Ye TJ, DeCaro E, Buehler B, Stahl Z, Bonavita G, et al. Intestinal SIRT1 Deficiency Protects Mice from Ethanol-Induced Liver Injury by Mitigating Ferroptosis. Am J Pathol 2020;190(1):82–92.
[21] Wang L, Zhang Z, Li M, Wang F, Jia Y, Zhang F, et al. P53-dependent induction of ferroptosis is required for artemether to alleviate carbon tetrachloride-induced liver fibrosis and hepatic stellate cell activation. IUBMB Life 2019;71(1):45–56.
[22] Na H, Lee H, Lee MH, Lim HJ, Kim HJ, Jeon Y, et al. Deletion of exons 3 and 4 in the mouse Nr1d1 gene worsens high-fat diet-induced hepatic steatosis. Life Sci 2016;166:13–19.
[23] Zhang H, Shi JH, Jiang H, Wang K, Lu JY, Jiang X, et al. ZBTB20 regulates EGFR expression and hepatocyte proliferation in mouse liver regeneration. Cell Death Dis 2018;9(5):462.
[24] Ferdinandusse S, Houten SM. Peroxisomes and bile acid biosynthesis. Biochim Biophys Acta 2006;1763(12):1427–40.
[25] Pironi L, Sasdelli AS. Intestinal Failure-Associated Liver Disease. Clin Liver Dis 2019;23(2):279–91.